

## Simultaneous Study of Elastic Scattering and Fusion in $^{16}\text{O} + ^{144}\text{Sm}$ : Success of Multi-Step Approximation Method

<sup>1</sup>P. K. Moharana<sup>1</sup>, C. Dash<sup>2</sup>, P. Mohanty<sup>2</sup>, G. Tripathy<sup>2</sup>, and B. B. Sahu<sup>2†</sup>

<sup>1</sup>Department of Physics, School of IKST, KISS Deemed to be University, Odisha-751024, INDIA

<sup>2</sup>Department of Physics

Maharaja Sriram Chandra Bhanj Deo University, Baripada-757003, INDIA

<sup>2</sup>Department of Physics, School of Applied Sciences,

KIIT, Deemed to be University, Odisha-751024, INDIA

\* email: [†bbsahufpy@kiit.ac.in](mailto:†bbsahufpy@kiit.ac.in)

### Introduction

Based on the optical model, simultaneous  $\chi^2$  analysis were performed on elastic scattering and fusion cross sections measured for the  $^{32}\text{S} + ^{58,64}\text{Ni}$  system at several energies around Coulomb barrier by Udagawa et. al. [1]. The imaginary potential used in this calculation consists of a surface type and a volume type fusion terms as  $W_D$  and  $W_F$  respectively, the latter of which accounts for fusion. They have explained elastic scattering cross section with energy dependent way and fusion cross section for large value of  $W_F$ . In [2], angular distribution of elastic scattering for the  $^{19}\text{F} + ^{208}\text{Pb}$  system have been measured at six different energies around Coulomb barrier. It is found that the real and imaginary part of the phenomenological optical potential show a pronounced energy dependence for the explanation of elastic scattering, in addition to this a large value of diffuseness parameter 'a' is required to explain the fusion cross section for this system. Further, accurate angular distributions of  $^{16}\text{O}$  ions scattered by  $^{58,60,62,64}\text{Ni}$  have been measured at five energies between 60 and 120 MeV by N. Keely et. al. [3]. They have also used the energy dependent potential and larger value of diffuseness parameter to explain fusion cross sections. The diffuseness parameter required to fit the high energy cross sections is higher than that required to fit elastic scattering data. Even the CC calculation failed to explain the oscillatory structure in barrier distribution function.

So by overcoming these difficulties we have successfully explained scattering

and fusion phenomena simultaneously with a unique potential. For this we have taken small diffuseness parameter 'a', deep real potential and very small imaginary potential to sustain resonance states. The details of the mathematics of multi-step approximation method are in Ref. [4, 5].

### Formulation

Here we adopt a convenient but somewhat different procedure to solve the schroedinger equation. Let us first consider the s-wave scattering in detail. A potential  $U(r)$  can be considered as a chain of n number of rectangular potentials, each of which has arbitrary small width w. In fact in any numerical integration of differential equation similar procedure is implicit. Having simulated the potential up to a maximum range of  $r = R_{\max}$ , we have  $R_{\max} = \sum_i^n w_i$ , where  $w_i = w$  is the width of the  $i^{\text{th}}$  rectangle.

The reduced Schroedinger equation in this region is

$$\frac{d^2\phi(r)}{dr^2} + \frac{2m}{\hbar^2}(E - U_j)\phi(r) = 0 \quad (1)$$

With the following solution

$$\phi_j(r) = a_j e^{ik_j r} + b_j e^{-ik_j r} \quad (2)$$

Total absorption or reaction cross section in the region  $0 < r < R_n$  is given by

$$\sigma_{\text{abs}}^{(0)} = \frac{\pi}{k^2} \left( 1 - \frac{|a_n|^2}{|b_n|^2} \right) \quad (3)$$

Where

$$1 - \frac{|a_n|^2}{|b_n|^2} = \sum_{j=1}^n I_j$$

$I_j$  represents absorption cross section as discrete sums of contributions from various sections.

This result in  $j^{\text{th}}$  segment can be expressed as

$$I_j = \left( -\frac{1}{k_n} \right) \frac{\text{Im}U_j}{|b_n|^2} \left\{ \begin{array}{l} \frac{|b_j|^2}{2\text{Im}k_j} e^{-2\text{Im}k_j w_{j-1}} (e^{2\text{Im}k_j w_j} - 1) \\ - \frac{|b_j|^2}{2\text{Im}k_j} e^{2\text{Im}k_j w_{j-1}} (e^{-2\text{Im}k_j w_j} - 1) \\ + \frac{1}{\text{Re}k_j} \text{Im}[a_j b_j^* e^{2\text{Im}k_j w_{j-1}} (e^{2i\text{Re}k_j w_j} - 1)] \end{array} \right\} \quad (4)$$

So the absorption (fusion) cross section in  $j^{\text{th}}$  region is given by

$$\begin{aligned} \sigma_{abs} &= \frac{\pi}{k^2} \sum_l (2l+1) \left( 1 - \frac{|\alpha_n|^2}{|b_n|^2} \right) \\ &= \frac{\pi}{k^2} \sum_l (2l+1) \left[ \sum_{j=1}^n I_j^{(l)} \right] \end{aligned} \quad (5)$$

### Results and Discussions

The formulation developed in the above section is applied to  $^{16}\text{O}+^{144}\text{Sm}$  system to analyze the collision data, to obtain a unified and consistent description and measurement of elastic scattering and fusion cross sections as well as to study the peculiar peak structure in the

variation of the quantity  $D(E_{c.m.}) = \frac{d^2(E_{c.m.} \cdot \sigma_{fus})}{dE_{c.m.}^2}$  as a function of  $E_{c.m.}$ . The optical parameters that is used in this calculation are  $V_N=100$  MeV,  $r_V=1.295$  fm,  $a_V=0.365$  fm,  $W=4.0$  MeV,  $r_W=1.25$  fm,  $a_W=0.15$  fm,  $r_C=1.1$  fm,  $V_B=60.25$  MeV,  $R_B=11.46$  fm,  $R_{fus}=10.0$  fm.

In Fig. 1, and 2 we compare our calculated results (solid curves) of differential scattering and fusion cross section with the corresponding experimental data (solid dots) taken from Refs. [6] at several energies. It is seen that the agreement with experimental data is quiet good. we obtain the results of the quantity  $D(E_{c.m.})$  as a function of  $E_{c.m.}$  for this system in Fig.3. It is seen that the main peak along with some smaller peaks in the higher energy region are well reproduced by our calculation.

### References

- [1] T. Udagawa, et al., *Phys. Rev. C* **39** (1989) 1840.  
 [2] C. J. Lin, et al., *Phys. Rev. C* **63** (2001) 064606.

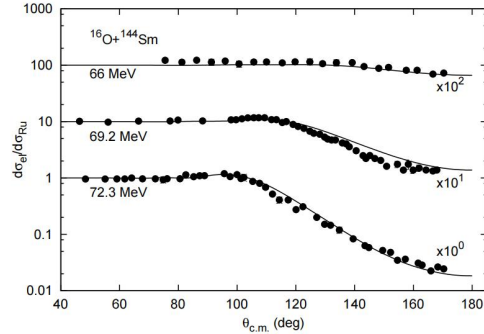


Fig.1: Angular distribution of elastic scattering cross sections (ratios to Rutherford) At different laboratory energies.

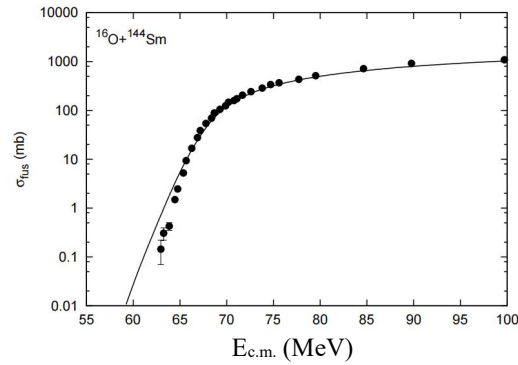


Fig.2: Variation of fusion cross section  $\sigma_{fus}$  as function of energy  $E_{c.m.}$ .

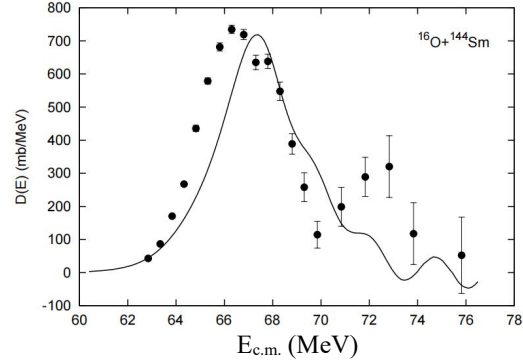


Fig.3: Variation of  $D(E)$  as a function of energy  $E_{c.m.}$ .

- [3] N. Keeley, et al., *Nucl. Phys. A* **582** 314.  
 [4] Basudeb Sahu, B.B. Sahu and S.K. Agarwal, *Pramana; J. Phys.* **70**, 27 (2008)  
 [5] Basudeb Sahu et al, *Phys. Rev. C* **77**, 024604 (2008)  
 [6] D. Abriola et. al., *Phys. Rev. C* **39** 546 (1989).